[1]L. D. Landau, J. Phys. USSR 5, 71 (1941); 11, 91 (1947).

[2]For a brief survey of recent literature on the excitation spectrum of superfluid helium see, for example, A. Zawadowski, J. Ruvalds, and J. Solana, Phys. Rev. A 5, 399 (1972). This reference is referred to as ZRS in the text.

[3]See, for example, A. D. B. Woods and R. A. Cowley, Can. J. Phys. 49, 177 (1970).

[4]J. Ruvalds and A. Zawadowski, Phys. Rev. Letters 25, 333 (1970)..

[5]L. D. Landau and I. M. Khalatnikov, in *Collected Papers of L. D. Landau*, edited by D. Ter Haar (Gordon and Breach, New York, 1967), pp. 494 and 511; I. M. Khalatnikov, *Theory of Superfluidity* (Benjamin, New York, 1965), p. 47.

[6]T. J. Greytak, R. Woerner, J. Yan, and R. Benjamin, Phys. Rev. Letters 25, 1547 (1970); T. J. Greytak and J. Yan, in *Proceedings of the Twelfth International Conference on Low-Temperature Physics*, edited by E. Kanda (Academic of Japan, Kyoto, 1969), p. 89.

[7]F. Iwamoto, Progr. Theoret. Phys. (Kyoto) 44, 1135 (1970).

[8]T. J. Greytak and James Yan, Phys. Rev. Letters 22, 987 (1969).

[9]Joseph Yau and M. J. Stephen, Phys. Rev. Letters 27, 482 (1971).

[10]I. A. Fomin, Zh. Eksperim. i Teor. Fiz. 60, 1178 (1971) [Sov. Phys. JETP 33, 637 (1971)].

[11]K. Nagai, K. Nojima, and A. Hatano, Progr. Theoret. Phys. (Kyoto) 46, 355 (1972).

[12]F. Toigo, Nuovo Cimento 62B, 103 (1969).

[13]J. Solana, thesis (University of Virginia, 1971) (unpublished).

[14]A. A. Abrikosov, L. P. Gorkov, and I. E. Dzyaloshinski, *Methods of Quantum Field Theory in Statistical Physics* (Prentice-Hall, Englewood Cliffs, N. J., 1963).

[15]Our result for $\rho_2^{(0)}$ differs by a factor of 2 from the Landau-Khalatnikov formula; their work contains an error neglecting the indistinguishability of the rotons. It should be noted that Eq. (2.9) is valid only for $\omega \simeq 2\Delta_0$. However, the corrections to $\rho_2^{(0)}$ yield an insignificant contribution to the roton lifetime (see Ref. 13). Also, $\rho_2^{(0)}$ is more complicated for very small values of the total momentum (see Ref. 2); however, these complications do not affect the roton lifetime.

[16]R. P. Feynman and M. Cohen, Phys. Rev. 102, 1189 (1956).

[17]I. Tüttö (unpublished).

[18]V. Celli and J. Ruvalds, Phys. Rev. Letters 28, 539 (1972).

[19]O. W. Dietrich, E. H. Graf, C. H. Huang, and L. Passell, Phys. Rev. (to be published).

[20]J. Ruvalds, Phys. Rev. Letters 27, 1769 (1972).

PHYSICAL REVIEW A VOLUME 6, NUMBER 4 OCTOBER 1972

Electrohydrodynamic Solutions for the Homeotropic Nematic-Liquid-Crystal Geometry

P. Andrew Penz*
Scientific Research Staff, Ford Motor Company, Dearborn, Michigan 48121

and

G. W. Ford
Department of Physics, University of Michigan, Ann Arbor, Michigan 48104

(Received 5 April 1972)

We have solved the boundary-value problem associated with the electro-optic mode which appears in a nematic liquid crystal subjected to a dc electric field parallel to the nematic director. Above a critical voltage, the liquid breaks up into a series of cylindrical lenses similar to those observed in the Williams domain mode. The dispersion relations for *p*-azoxyanisole and *p*-methoxybenzylidene-*p*-*n*-butylaniline were calculated using the known material constants for these two nematogens. We show that the critical voltage is caused by the dielectric torque opposed by the bend distortion torque; the critical voltage is not sensitive to the various viscosity parameters nor the conductivities. The dispersion relation at higher voltages does involve these constants.

I. INTRODUCTION

Electro-optic effects in nematic liquid crystals (NCL) have been an area of intense study in the past several years due to their inherent interest and to the possibility of practical application. While early work had given clear indication of electro-optic effects, the current activity began with the work of Williams.[1] Williams used what has become the standard experimental geometry: a sandwich capacitor with at least one transparent electrode and a NLC for the thin dielectric layer. Unless the surfaces of the capacitor are specially treated, the nematic director will lie in the plane of the capacitor. In this *perpendicular* geometry the director and electric field are orthogonal. Williams found that when the NLC was subjected to a dc electric field, it exhibited a visible line texture which has since become known as the Williams domain mode (WDM). Heilmeier, Zanoni,

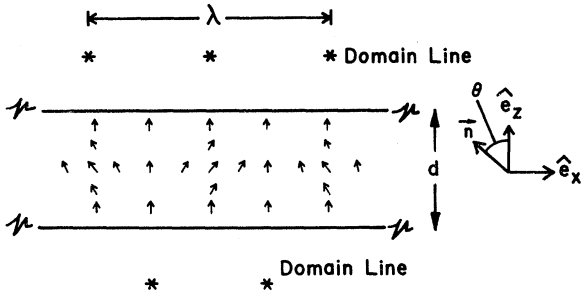

FIG. 1. Model of the director distortion pattern consistent with the homeotropic boundary conditions ($V > V_c$). The NLC is confined between two transparent electrodes at $z = \pm\frac{1}{2}d$, where d is the capacitor thickness. The arrows in the figure represent the orientation of the director $\vec{n}$ at the position of the arrow. The angle the director makes with respect to the z direction is $\theta \sim \theta_1 e^{i\vec{q}\cdot\vec{r}}$. The pattern has a wavelength of $\lambda = 2\pi/q_x$ in the x direction. The x direction has been defined by rubbing the capacitor plates. Due to the anisotropy of the index of refraction associated with the NLC, this pattern can be thought of as a series of cylindrical lenses, the axes of the cylinders being parallel to the figure, i.e., the y direction. The center of the director pattern represents an optical-path maximum. If light is directed at the sample from below and observed from above, there will be a real image formed over the center of this pattern. The edges of the pattern are an optical-path minimum and virtual images will be formed below the samples. These line images are shown in cross section in the figure, and have been labeled as domain lines in analogy to the WDM. The solution of the theoretical problem is a prediction of λ as a function of the applied voltage. The figure is drawn circular, $\pi d/\lambda = \frac{1}{2}\pi$, although in general the distortions are elliptical.

and Barton[2] demonstrated the device capability of the perpendicular geometry. At higher voltages the line texture becomes very time dependent, leading to strong light scattering. This turbulent regime has become known as the dynamic-scattering mode (DSM). A third mode has been observed using the perpendicular geometry in very thin (5-μm) samples. Greubel and Wolff[3] report that for such thin samples the density of the line texture increases linearly with voltage. Since the domain line spacing is in the right region for diffraction of visible light, this mode corresponds to a voltage variable-diffraction grating. We have suggested the name variable-grating mode (VGM) to describe this phenomenon.[4] Vistin[5] has also reported observing similar effects in the perpendicular geometry.

It is possible to prepare samples where the nematic director lies perpendicular to the surface of the capacitor. Greubel and Wolff[3] report achieving this result by coating the surface with lecithin. Thus the director and the electric field are parallel in this configuration which we will refer to as the *parallel* geometry. Schiekel and Fahrenschon[6] report obtaining this *homeotropic* geometry by special electrode-cleaning methods. The response of a homeotropic sample to an electric field is an experimental feature which seems to depend on sample conductivity and driving frequency. Greubel and Wolff report that a dc electric field produces a stable Williams domain texture at a critical voltage. Schiekel and Fahrenschon report that ac electric fields produce a constant deformation texture followed by the DSM at higher voltages, depending on frequency and conductivity. They have referred to the constant texture as the DAP mode. Others[7,8] have observed a constant deformation texture followed by a stable domain texture, again depending on frequency and conductivity. We suggest that the domain texture associated with the homeotropic geometry be named the homeotropic domain mode (HDM) in analogy with the WDM terminology.

II. THEORETICAL MODEL

We intend to discuss the HDM in a manner analogous to our treatment of the WDM/VGM.[9] We assume that the reader is familiar with Ref. 9 or is somewhat conversant with electrohydrodynamics. We approximate the three-dimensional problem by assuming a two-dimensional model for the spatial distribution of the director (Fig. 1) and the fluid flow lines (Fig. 2). The capacitor is shown in cross section, the z direction being that of the applied electric field and the initial direction of the undisturbed NLC. The appearance of uniform domain lines indicates that the sample distorts into the spatial distributions shown in Figs. 1 and 2. The x direction is defined by the director

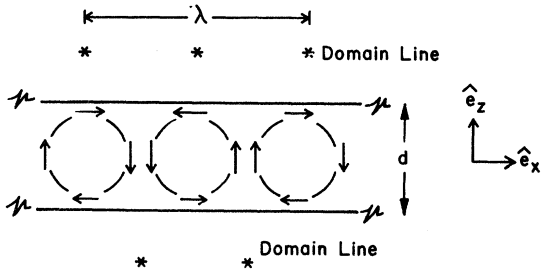

FIG. 2. Model of the fluid streamline pattern consistent with the homeotropic geometry ($V > V_c$). We expect that there will be vortex motion similar to that observed in the WDM. Adjacent vortices will have antiparallel vorticity. The vortex motion has the same wavelength as the lens distortion. The centers of the vortex motion will be directly under the real images, just the opposite from the WDM where the virtual images are under the centers of the vortex motion. It is shown in the paper that the critical voltage is strictly an electrostatic phenomenon. Thus it may be difficult to observe fluid motion, i.e., entropy production, close to threshold.

as it tips from the z direction; this can be promoted by rubbing the surfaces of the electrodes.[3] The domain lines are assumed to run for long distances in the y or third perpendicular direction. The tipping angle is measured by θ as shown in Fig. 1.

The forces and torques involved in the theoretical problem have been discussed by Helfrich.[10] The fluid motion is a direct result of the anisotropic conductivity tensor associated with the NLC. $\sigma_\perp$ and $\sigma_\parallel$ will be the Ohmic conductivities perpendicular and parallel to the director, respectively. A director pattern such as indicated in Fig. 1 will produce a net space charge which in turn can produce a local stress. The liquid crystal resists the electromechanical stress with a viscous shear stress associated with the shear-strain pattern indicated in Fig. 2. The viscosities η_1 and η_2 describe the anisotropic shear stress associated with strain rates when the flow is parallel and perpendicular to the director, respectively. There are several torques acting to turn the director. The shear flow produces a shear torque unique to liquid-crystal systems. The shear-torque "viscosities" α_2 and α_3 describe the constitutive relationship between the torque and strain rates. $\alpha_2+\alpha_3$ relates torque and the fluid motion; $\alpha_3-\alpha_2$ relates torque and director rotation relative to fluid vorticity. There are elastic torques associated with splay and bend distortions of the director, described by the elastic coefficients k_{11} and k_{33}, respectively. Finally, there is the electric torque associated with the anisotropic conductivity and dielectric constant tensors. $\epsilon_\perp$ and $\epsilon_\parallel$ are the dielectric constants perpendicular and parallel to the director, respectively. This electrohydrodynamic formulation of the electro-optic effects in NLC was first pioneered by Helfrich.[10] He identified the relevant physical parameters, and this paper should be regarded as an extension of his work to the solution of the boundary-value problem.

III. EQUATIONS OF MOTION IN INFINITE MEDIUM

The force, torque, and mass continuity equation have been discussed extensively in Ref. 9. The electric ponderomotive forces are represented by the Maxwell stress tensor, and the fluid equations follow the Leslie approach.[11] The electric fields are described by Maxwell's equations. The complete set of fluid-field equations involve several nonlinear terms. We have linearized the problem by the standard mathematical technique of considering small amplitude oscillations about the unperturbed state. Since the infinite medium problem is translationally invariant, the normal modes of the linear problem can be expected to be described by plane-wave functions: $e^{i\vec{q}\cdot\vec{r}}$, where $\vec{q}=(q_x,\ 0,\ q_z)$. The wave vector $\vec{q}$ is assumed not to have a component in the y direction since we will not discuss spatial variation in this direction. The Maxwell stress tensor is derived using a director of the form $\vec{n}=(-\theta_1 e^{i\vec{q}\cdot\vec{r}},\ 0,\ 1)$ and an electric field of the form

$$\vec{E}=(0,\ 0,\ 1)E_0+(1,\ 0,\ S)E_1 e^{i\vec{q}\cdot\vec{r}},$$

where $S=q_z/q_x$. Note that $\nabla\times\vec{E}=0$ and $|\vec{n}|=1$ to first order in θ_1. The fluid-stress tensor is derived using a pressure of the form $p=p_0+p_1e^{i\vec{q}\cdot\vec{r}}$ and a velocity of the form $\vec{v}=(-S,\ 0,\ 1)v_1e^{i\vec{q}\cdot\vec{r}}$. We assume steady-state conditions. Together with the linearity assumption, this means that all convective time derivatives are set equal to zero. The mass continuity equation reduces to $\nabla\cdot\vec{v}=0$, which can be seen to be true for the assumed velocity distribution; we are treating an incompressible fluid. We also assume that no temperature gradients are present, electrostriction effects are absent, and the gravitational potential is zero. The Leslie viscosity coefficient α_1 is assumed to be zero. The remaining constitutive parameters discussed in Sec. II have been measured experimentally and are given in Table I for p-azoxyanisole (PAA) and p'-methoxy-benzylidene-p-n-butylaniline (MBBA).

The infinite-medium problem reduces to a series of four linear homogeneous equations involving the amplitudes v_1, E_1, θ_1, and p_1. These equations can be solved only if the associated determinant is zero:

$$0=(S^2+1)\Bigg(S^6+S^4\left\{\frac{\eta_1}{\eta_2}+\frac{k_{11}}{k_{33}}+\frac{\sigma_\perp}{\sigma_\parallel}-\frac{E_0}{q_x}\frac{\epsilon_0(\epsilon_\perp-\epsilon_\parallel)}{k_{33}}\right\}$$

$$+S^2\left\{\frac{\eta_1}{\eta_2}\frac{k_{11}}{k_{33}}+\frac{\eta_1}{\eta_2}\frac{\sigma_\perp}{\sigma_\parallel}+\frac{k_{11}}{k_{33}}\frac{\sigma_\perp}{\sigma_\parallel}-\frac{E_0^2}{q_x^2}\frac{\epsilon_0}{k_{33}}\left[(\epsilon_\perp-\epsilon_\parallel)\left(\frac{\eta_1}{\eta_2}+1\right)-\left(\epsilon_\parallel\frac{\sigma_\perp}{\sigma_\parallel}-\epsilon_\perp\right)\frac{\alpha_2}{\eta_2}\right]\right\}$$

$$+\left\{\frac{1}{2}\frac{k_{11}}{k_{33}}\frac{\sigma_\perp}{\sigma_\parallel}-\frac{E_0^2}{q_x^2}\frac{\epsilon_0}{k_{33}}\left[\left(\epsilon_\parallel\frac{\sigma_\perp}{\sigma_\parallel}-\epsilon_\perp\right)\frac{\alpha_3}{\eta_2}-(\epsilon_\perp-\epsilon_\parallel)\frac{\eta_1}{\eta_2}\right]\right\}\Bigg). \qquad (1)$$

TABLE I. Experimental values of the material constants used for the calculating.

	MBBA (25 °C)	PAA	
k_{11}	6.10×10^{-12} N[a]	7×10^{-12} N[b]	120 °C
k_{33}	7.25×10^{-12} N[a]	17×10^{-12} N[b]	120 °C
$\epsilon_{\parallel}$	4.72[c]	5.62[d]	120 °C
$\epsilon_{\perp}$	5.25[c]	5.83[d]	120 °C
η_1	23.8×10^{-3} kg m^{-1} sec^{-1} [e]	1.5×10^{-3} kg m^{-1} sec^{-1} [f]	125 °C
η_2	103.5×10^{-3} kg m^{-1} sec^{-1} [e]	8.6×10^{-3} kg m^{-1} sec^{-1} [f]	125 °C
α_2	-77.5×10^{-3} kg m^{-1} sec^{-1} [e]	-6.4×10^{-3} kg m^{-1} sec^{-1} [f]	125 °C
α_3	-1.2×10^{-3} kg m^{-1} sec^{-1} [e]	-0.6×10^{-3} kg m^{-1} sec^{-1} [f]	125 °C
$\sigma_{\parallel}/\sigma_{\perp}$	1.5[c]	1.5[g] (estimate)	

[a]Reference 12.
[b]Reference 13.
[c]Reference 14.
[d]Reference 15.
[e]Reference 16.
[f]Reference 17.
[g]Reference 18.

We have used a rationalized system of mks units, and so the permittivity of free space, ϵ_0, enters this infinite-medium dispersion relation. Equation (1) is an eighth-order algebraic equation in S with a parameter E_0/q_x. In general there are eight solutions to such an equation; two solutions $S=\pm i$ are readily apparent. Thus we expect to have eight possible plane-wave states for each E_0/q_x. Helfrich's solution corresponds exactly to the limit of Eq. (1) as S goes to zero. (It should be remembered that Helfrich's treatment interchanged the standard definitions of η_1 and η_2.)

IV. BOUNDARY-VALUE PROBLEM

The infinite-medium dispersion relation has shown that there is a continuum of wave vectors q_x which solve the equations of motion. For a given q_x and E_0, there are eight possible values of q_z. The imposition of boundary conditions on a harmonic problem possessing a continuous spectrum usually produces a discrete pattern of normal modes. We now introduce boundary conditions and show that for a given voltage V_0 and a sample thickness d, the spectrum of q_x is discrete.

There are four physical requirements for the distortion amplitudes at each electrode, i.e., eight boundary conditions. The fluid must remain inside the capacitor, and thus, $v_z(z=\pm\frac{1}{2}d)=0$. The fluid flow parallel to the plates must be zero at the plates to avoid infinite viscous loss, and thus $v_x(z=\pm\frac{1}{2}d)=0$. Since the capacitor plates are good conductors relative to the liquid crystal, the electric field can have no x component at the plates: $E_x(z=\pm\frac{1}{2}d)=0$. Finally, we assume that the surface treatment has been such to constrain the molecules to lie perpendicular to the surface. For the HDM, $n_x(z=\pm\frac{1}{2}d)=0$. In a previous paper,[9] we have treated the complementary boundary condition, i.e., the director constrained to lie in the plane of the capacitor faces.

The problem we are considering is bounded only in the z direction. From symmetry considerations, we expect the normal modes of the bounded problem to still be plane waves with respect to their x dependence, i.e., of the form $f_\alpha(z)e^{iq_x x}$. The functions f_α, representing the z dependence of v_x, v_z, n_x, and E_x, must have the symmetry of the boundary conditions. We form linear combinations of the eight infinite-medium solutions to achieve the constraints put on the problem by the eight boundary conditions in the z direction.

We note that the boundary conditions are symmetric about $z=0$ and that the values of S come in $\pm$ pairs [Eq. (1) is a quadratic equation in S^2]. The boundary-value problem can thus be separated into two complementary problems (each involving only four boundary conditions) with sine and cosine functions of z. For instance, the two components of velocity *at the boundary* can be described by

$$e^{iq_x x}\sum_{j=1}^{4} {}^{j}v_{1\,\cos S_j\varphi} \quad \text{or} \quad e^{iq_x x}\sum_{j=1}^{4} {}^{j}v_{1\,\sin S_j\varphi},$$

where $\varphi\equiv\frac{1}{2}q_x d$ and ${}^{j}v_1$ are amplitudes to be determined by the boundary conditions. The other three physical variables can be similarly constructed from sine and cosine functions, the coefficients always involving the four unknown amplitudes ${}^{j}v_1$. The boundary-value problem reduces to two sets of linear homogeneous equations involving the amplitudes ${}^{j}v_1$. Naturally, such a set of equations can only be solved if the determinant is equal to zero. We reproduce one of the two boundary-value determinants (BVD) below:

$$\begin{vmatrix} \cos S_1\varphi, & \cos S_2\varphi & \cos S_3\varphi & \cos S_4\varphi \\ S_1\sin S_1\varphi & S_2\sin S_2\varphi & S_3\sin S_3\varphi & S_4\sin S_4\varphi \\ M_1\cos S_1\varphi & M_2\cos S_2\varphi & M_3\cos S_3\varphi & M_4\cos S_4\varphi \\ M_1N_1\cos S_1\varphi & M_2N_2\cos S_2\varphi & M_3N_3\cos S_3\varphi & M_4N_4\cos S_4\varphi \end{vmatrix} = 0, \tag{2}$$

where

$$M_i=\left(\frac{\alpha_3}{\alpha_2}-S_i^2\right)\Big/\left[\frac{\epsilon_0E_0^2}{q_x^2}\,\frac{\epsilon_\perp-\epsilon_\parallel}{k_{33}}\,(1+S_i^2)-\left(\frac{k_{11}}{k_{33}}+S_i^2\right)\left(\frac{\sigma_\perp}{\sigma_\parallel}+S_i^2\right)\right], \qquad N_i=\sigma_\perp/\sigma_\parallel+S_i^2.$$

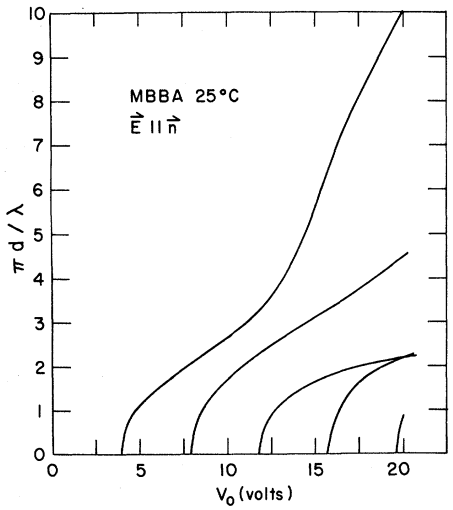

FIG. 3. Computer calculation of the normal-mode structure of MBBA at 25 °C. The curves in the figure are the only points in the $\pi d/\lambda$, V_0 plane for which Eqs. (1) and (2) or its dual equation are simultaneously satisfied. The phase factor $\pi d/\lambda$ is discrete at any given applied voltage V_0. There is a critical voltage of 3.98 V for HDM. It is shown in the paper that this critical voltage can be well approximated by the formula $V_c = 3.21\ [k_{33}/\epsilon_0(\epsilon_\perp - \epsilon_\parallel)]^{1/2}$ except near $\epsilon_\perp = \epsilon_\parallel$. The distortion begins at infinite wavelength and the pattern becomes circular at about 7 V. At still higher voltages, the pattern becomes elongated in the z direction. It can be seen that another mode becomes possible at 8 V. This mode results from the simultaneous solution of Eq. (1) and the dual of Eq. (2). Physically it represents two layers of vortex/lens distortions. It is argued in the text that turbulence may be expected at 8 V due to the interference of the single- and double-layered solutions. The dispersion curves of three-, four-, and five-layer patterns are also shown. The experimental values of the physical constants used in the calculation are given in Table I. While the critical voltage is an electrostatic phenomenon, the detailed shape of the dispersion curves above threshold has been shown to depend upon $\sigma_\parallel/\sigma_\perp$, k_{11}/k_{33}, and α_2/η_2. It should be emphasized that there are no undetermined constants in this theory to be adjusted to fit experiments. Nonlinear and time-dependent effects might cause quantitative differences between experiments and this linear steady-state theory.

The complementary BVD is obtained by interchanging sines and cosines in Eq. (2). The boundary-value problem is solved for those values of V_0, d, and q_x for which both Eqs. (1) and (2) (or the complementary BVD) are solved.

The actual solution of the problem must be done numerically. We will give only a brief discussion of the method. Copies of the program can be obtained by request. We note that Eq. (1) involves a function of the ratio $E_0/q_x = V_0/2\varphi$. We chose a value for V_0 and φ. The four values of S^2 are determined and the BVD is evaluated. In general, the BVD will not be zero, i.e., a general V_0, φ combination will not solve the problem. A systematic search of the V_0, φ plane is performed numerically. The values of V_0 and φ for which either BVD is zero are given in Fig. 3 for MBBA and in Fig. 4 for PAA. For a more complete discussion of the general method, we refer the reader to Ref. 9.

V. NUMERICAL SOLUTIONS

The "dispersion relations" describing the normal modes of the MBBA and PAA systems are shown in Figs. 3 and 4, respectively. The material constants used in the calculations are given in Table I. Several qualitative features are common to both figures. There are a series of dispersion curves, each beginning at a critical voltage. Below 4 V, no distortions in the homeotropic texture will occur. At 4 V, a distortion with zero-phase factor becomes possible. The zero-phase factor corresponds to an infinite wavelength, i.e., a uniform spatial texture. We interpret this threshold behavior as being responsible for the observation of Schiekel and Fahrenschorn.[6] As the voltage across the sample is increased, the wavelength of the pattern decreases so that a line texture should become observable. The vortex structure will be circular at roughly 7 V. Greubel and Wolff[3] have reported such a line texture when an electric field is applied to the homeotropic geometry. As the voltage is further increased, the cell structure will again be elliptical with the semiminor axis in the x direction. Since the wavelength depends on voltage, the HDM possesses the same tunable-grating possibility as has been observed in the VGM.[3]

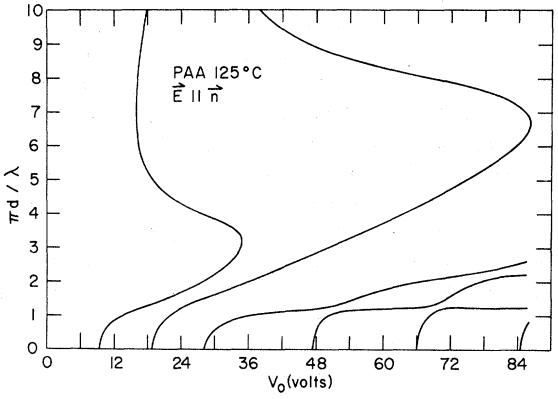

FIG. 4. Computer calculation of the normal-mode structure of PAA near 125 °C (see Table I for the physical constants). The general nature of the solutions is similar to the features discussed in Fig. 3. The modes for one, two, three, five, seven, and nine layers of vortex/lens patterns are shown. The four, six, and eight modes have been omitted for clarity. It can be seen that the one and two modes become multivalued functions of V_0. The significance of this fact is not known.

Some care must be taken when comparing these calculations with experiment. First of all, we have assumed that the director is rigidly oriented perpendicular to the surfaces at the surfaces, even in the presence of the electric field. The physical reality may be somewhat different. Most experiments are performed with ac voltages in order to avoid chemical polarization effects at the electrodes.[19] The calculations are done assuming a dc voltage, although the results should be applicable to low-frequency measurements. The electrical stresses are quadratic in the field strength[9,19] and a net rms stress is produced. The effect of frequency changes on the detailed shape of the dispersion relations remains to be determined. Finally, the calculations were performed using a linearized theory. Above threshold, nonlinear terms will determine the amplitude of the distortion. The linearized dispersion relations in Figs. 3 and 4 are expected to change somewhat as nonlinear effects are included. Experiments have shown the linear approximation to be fairly good in the WDM.[9] It remains to be seen how well the approach will work in the HDM.

Figure 3 shows that another MBBA dispersion relation beings at 8 V. Computer investigation of the velocity profiles reveals that this branch corresponds to two layers of vortex motion. Each higher solution, at roughly an integer multiple of the single-layer threshold voltage, describes a pattern containing one additional vortex/lens layer. Figure 3 shows dispersion curves for five vortex layers.

The phase factor $\pi d/\lambda$ is the ordinate for both Figs. 3 and 4. As the sample thickness changes, the wavelength associated with the pattern at a given voltage will follow linearly. This behavior is well established for the WDM and should be easily verified for this mode. It should also be noted that in Fig. 2 the top domain lines are over the centers of the vortex motion. Exactly the opposite is observed for the WDM. This prediction should also be easily verified. The reason for the difference between the two geometries regarding the domian positions is the interchange of the indices of refraction in the formula describing the optical-path length.[19]

Figure 3 shows that at 9 V both single and double layers of vortices simultaneously satisfy the boundary-value problem for MBBA. Our analysis has been a steady-state linear treatment and so we cannot predict the relative stability of the two possible solutions. It is well known in the field of stability analysis that turbulence may be expected when a stationary solution has superposed on it a small perturbation.[20] On such experience we can base a conjecture that the superposition of the two layer solution on the one layer solution will lead to turbulence. There is experimentally observed turbulence.[3]

The PAA dispersion curves show considerably more variety in their patterns than the MBBA modes. It can be seen in Fig. 4 that the single-layer solution becomes multivalued at approximately 18 V. The double-layer solution exhibits a similar behavior. Figure 4 presents the odd-layer solutions one–nine; the even layer solutions four–eight have been suppressed for clarity. As was stated above, we have not treated the stability problem and so are not able to discuss rigorously the influence of the multivalued dispersion relations for PAA.

It is possible to compute the spatial variation of the $\vec{v}$, $\vec{E}$, and θ fields associated with the normal modes in Figs. 3 and 4. These computer calculations confirm the one-, two-, etc. layer nature of the mode system. The theoretical distributions are very much like those shown in Fig. 4 of Ref. 9. We will not, therefore, present such a figure here.

VI. PARAMETER VARIATION

Computer calculations of electrohydrodynamic effects are not limited to the parameters associated with any particular physical system. We have performed some preliminary evaluation of the homeotropic mode structure when the various constitutive parameters are systematically varied. The first feature of the mode system we investigated was the threshold voltage of 3.98 V for MBBA. To within an accuracy of 0.1 V, the threshold voltage is independent of the following parameters when they are changed by 100% or more: η_1/η_2, α_2/η_2, α_3/η_2, $\sigma_\perp/\sigma_\parallel$, and k_{11}/k_{33}. This result implies that the threshold condition does not involve conduction-induced torque or fluid motion. The critical voltage can be represented by the formula

$$V_c = 3.21\left(\frac{k_{33}}{\epsilon_0(\epsilon_\perp - \epsilon_\parallel)}\right)^{1/2}, \qquad \epsilon_\parallel \neq \epsilon_\perp . \tag{3}$$

The formula does not hold at the isotropic dielectric-constant limit where the computer calculation reveals a finite threshold voltage of 23 V. For $\epsilon_\perp/\epsilon_\parallel \geq 1.01$, however, the formula does give 1% accuracy. Calculations show V_c becomes arbitrarily large for slightly positive dielectric anisotropies ($\epsilon_\perp/\epsilon_\parallel > 1$).

The physical interpretation of the voltage dependence has been known for at least 40 years.[21] The mechanism is a pure dielectric torque due to the dielectric anisotropy being opposed by an elastic torque associated with a bend distortion as in Fig. 1. Similar formulas have appeared recently for the distortion of cholesterics by electric and magnetic fields.[22,23] The subtle part of the present problem is to predict again the characteristic

length in the x direction. The simplicity of the physical situation makes it possible to argue why one might expect a periodic distortion. The director associated with a NLC does not have a positive or negative sense. Thus the torques at threshold would equally prefer a positive or negative θ in Fig. 1. Nature appears to compensate for the degeneracy by alternating the sign of θ, i.e., by producing a pattern with an x dependence.

The simple form of Eq. (3) can be deduced from Eq. (1) once the boundary-value problem has been solved. The numerical analysis reveals that one of the four values of S^2 is a large positive number ($S^2 \sim 60$). Equation (1) can be reduced to a "voltage"-type condition if one assumes that S^2 is a large number:

$$\frac{E_0}{q_x} = \left(S^2 \frac{k_{33}}{\epsilon_0(\epsilon_\perp - \epsilon_\parallel)} \right)^{1/2}, \quad S^2 \gg 1. \tag{4}$$

This should be compared with Helfrich's "voltage"-type condition under his *assumption* that $S = 0$ was a good physical approximation to Eq. (1):

$$\frac{E_0}{q_x} = \left\{ k_{11} \Big/ \left[\epsilon_0 \epsilon_\perp \left(\frac{\epsilon_\parallel}{\epsilon_\perp} - \frac{\sigma_\parallel}{\sigma_\perp} \right) \frac{\alpha_3}{\eta_1} + \epsilon_0 (\epsilon_\perp - \epsilon_\parallel) \frac{\sigma_\parallel}{\sigma_\perp} \right] \right\}^{1/2}, \quad S^2 = 0. \tag{5}$$

The two formulas are grossly different in their physical interpretation. This shows the necessity for a rigorous solution of the boundary-value problem if meaningful comparison is to be made between experiment and theory.

Equation (3) is a relationship between an experimentally measurable number, V_c, and two constitutive constants, k_{33} and $\epsilon_\perp - \epsilon_\parallel$. As such, it offers a measure of the ratio $k_{33}/(\epsilon_\perp - \epsilon_\parallel)$. This means that electrohydrodynamic phenomena in NLC are sufficiently well understood to permit measurements of the associated material constants. There is a wealth of other information in the dispersion curves, and it might be possible to measure other material parameters by simply measuring the line spacing as a function of voltage. We have found that a variation of $\sigma_\parallel/\sigma_\perp$, k_{11}/k_{33}, and α_2/η_2 produces a change in the detailed shape of the dispersion relation above threshold. This means that some conduction-induced shear is beginning to produce flow. Within a few volts above threshold, α_3/η_2 and η_1/η_2 have very little influence on the shape of the dispersion relation. Naturally, a more extensive study of the experimental and theoretical sensitivities would be necessary to test the feasibility of such a measurement technique.

VII. REMARKS ON TIME-DEPENDENT PROBLEM

We have discussed the electrohydrodynamic problem under the assumptions of *linearity* and *steady state*. As a result, we cannot make predictions about the stability of the patterns obtained. To do this we must treat the time-dependent linearized problem, assuming a time dependence of the form $e^{-i\omega t}$. The condition that the boundary-value determinants vanish then becomes a relation between ω and q_x, which is to be solved for complex ω as a function of real q_x. Those values of q_x for which $\omega(q_x)$ has a positive imaginary part correspond to exponentially growing patterns whose ultimate amplitude will be determined by nonlinear effects. This means that there is a possibility for bands of q_x, V_0 for which solutions exist, rather than the line solutions as in Figs. 3 and 4. What we have done in this present paper is to find the values of q_x for which $\omega(q_x) = 0$. Since the patterns observed experimentally are *stationary* and have small amplitudes,[19] one would expect they would correspond to the linearized steady-state solutions we have found. The time-dependent problem will be the subject of a later paper.

VIII. CONCLUSIONS

We have solved the boundary-value problem associated with a two-dimensional distortion of a homeotropic NLC subjected to a dc electric field. We find that there are HDM solutions corresponding to the WDM/VGM in the director field-perpendicular geometry. The distortions begin at a critical voltage which is primarily caused by an electrostatic interaction. Above threshold conductivity effects become noticeable. The distortion pattern begins at infinite wavelength and decreases in wavelength as the voltage is increased. We have shown how experimental measurements can be used to measure $k_{33}/(\epsilon_\perp - \epsilon_\parallel)$ and indicated that other parameters may also be obtainable.

ACKNOWLEDGMENTS

The authors wish to thank Dr. W. Weber for assistance. They are also grateful for the MBBA values of k_{11} and k_{33} supplied by I. Haller in the numerical calculations.

---

*Present address: Research Laboratory, Texas Instruments Inc., Dallas, Tex. 75222.

[1]R. Williams, J. Chem. Phys. 39, 384 (1963).

[2]G. H. Heilmeier, L. A. Zanoni, and L. A. Barton, Proc. IEEE 56, 1162 (1968).

[3]W. Greubel and U. Wolff, Appl. Phys. Letters 19, 213 (1971).

[4]P. A. Penz and G. W. Ford, Appl. Phys. Letters 20, 415 (1972).

[5]L. K. Vistin, Kristallografiya 15, 594 (1970) [Sov.

Phys. Crystallogr. 15, 514 (1970)].
[6]M. F. Schiekel and K. Fahrenschon, Appl. Phys. Letters 19, 391 (1971).
[7]H. Bücher (private communication).
[8]A. Kmetz (private communication).
[9]P. A. Penz and G. W. Ford, Phys. Rev. 6, 414 (1972).
[10]W. Helfrich, J. Chem. Phys. 51, 4092 (1969).
[11]F. M. Leslie, Quart. J. Mech. Appl. Math. 19, 357 (1966).
[12]I. Haller (private communication).
[13]A. Saupe, Z. Naturforsch. 15a, 815 (1960).
[14]D. Diguet, F. Rondelez, and G. Durand, Compt. Rend. 271B, 954 (1970).
[15]W. Maier and G. Meier, Z. Naturforsch. 16a, 470 (1961); 16a, 1200 (1961).
[16]C. Gähwiller, Phys. Letters 36A, 311 (1971); we have interchanged the definitions of η_1 and η_2 used in this reference.
[17]Orsay Liquid Crystal Group, Mol. Cryst. 13, 187 (1971).
[18]R. P. Twitchell and E. F. Carr, J. Chem. Phys. 46, 2765 (1967).
[19]P. A. Penz, Mol. Cryst. 15, 141 (1971).
[20]L. D. Landau and E. M. Lifshitz, *Fluid Mechanics* (Pergamon, London, 1959), p. 102.
[21]See, for instance, V. Freedericksz and V. Zolina, Trans. Faraday Soc. 29, 919 (1933); H. Zocher, *ibid.* 19, 945 (1933).
[22]P. G. de Gennes, Solid State Commun. 6, 163 (1968).
[23]R. B. Meyer, Appl. Phys. Letters 12, 281 (1968).